Communication

Marangoni Flow-Induced Self-Assembly of Hexagonal and Stripelike Nanoparticle Patterns

Yangjun Cai, and Bi-min Zhang Newby

J. Am. Chem. Soc., **2008**, 130 (19), 6076-6077 • DOI: 10.1021/ja801438u • Publication Date (Web): 22 April 2008

J|A|C|S
COMMUNICATIONS

Published on Web 04/22/2008

Marangoni Flow-Induced Self-Assembly of Hexagonal and Stripelike Nanoparticle Patterns

Yangjun Cai and Bi-min Zhang Newby*

Department of Chemical and Biomolecular Engineering, The University of Akron, Akron, Ohio 44325-3906

Received February 26, 2008; E-mail: bimin@uakron.edu

Ordered nanoparticle (NP) assembly is of great interest in miniaturized devices, sensors, and high-density data storage.[1] One main challenge is to assemble NPs in desired locations exhibiting ordered patterns via a simple process. A number of approaches have been developed,[2] and evaporation-induced self-assembly has emerged as an elegant "bottom up" method and receives much attention.[2e–k] In the previous studies, ordered stripelike patterns (1-D) have been self-assembled[2g,h] but not the 2-D NP patterns.[3]

In this study, we report the spontaneous formation of ordered NP patterns by the Marangoni flow of ethanol into water, or the "tears of wine" phenomenon. In particular, hexagonal (2-D) and stripe like (1-D) polystyrene NP (100 nm) patterns (Figure 1) are formed on two types of SiO_x substrates, one with a water contact angle of ~32° (A) and the other of ~0° (B).

The formation of these patterns is the result of ethanol evaporation, water condensation, Marangoni flow, and subsequent drying and/or dewetting of the condensed water. When a small quantity (~1 μL) of NPs/ethanol suspension is spread into a thin layer on the substrate and exposed to a stream of wet N_2, volatile ethanol evaporates most near the air/ethanol/substrate contact line, which induces a maximum temperature decrease. As a result, water condenses near the contact line from the wet N_2 simultaneously (Figure 2a). This leads to a lower concentration of ethanol near the contact line compared with the bulk, and hence, a concentration gradient forms between the bulk and contact line (Figures 2b). Combined with the large difference between the surface tensions of water (72 mN/m) and ethanol (22 mN/m), a surface tension gradient is created, which induces a Marangoni flow of ethanol, carrying NPs, toward the contact line and into the water phase.[4] Due to its higher volatility, ethanol depletes faster than water, leaving the condensed water, containing NPs, at the edge of the contact line (Figure 2b). As the condensed water dries, the ordered NP patterns form on the substrate.

Depending on the wettabilities of the substrates, the condensed water consisting of NPs self-assembles into different patterns near the contact line. On the nonwettable substrate (i.e., substrate A), the formation of a hexagonal pattern is initiated by the fingering instability of the condensed water.[2g,5] Water fingers form at the air/ethanol/substrate contact line, grow, and detach to form droplets as the contact line recedes (Figure S1). The detached water droplets show a hexagonal distribution, which results from a phase shift of half of the wavelength of emerged fingers from one row to another (Figure S2). The water droplet, initially elongated, quickly relaxes into a spherical cap to minimize its surface energy. As the droplet relaxes, the inward capillary force drives the NPs to flow with the receding contact line of the water droplet.[2f] Thus, all NPs are confined in the

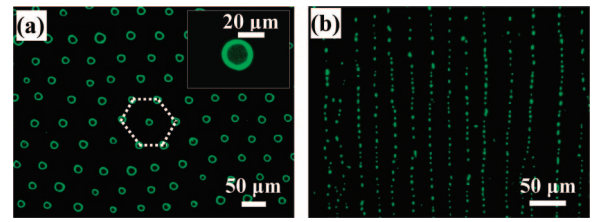

Figure 1. Fluorescent microscopic images of carboxylated PS NP self-assembly patterns. (a) Ordered hexagonal ring pattern formed on the SiO_x substrate A (water contact angle ~ 32°). Inset: magnified image of the NP ring structure. (b) Dotted stripelike pattern formed on the SiO_x substrate B (water contact angle ~ 0°). Humidity of N_2 stream = ~40%.

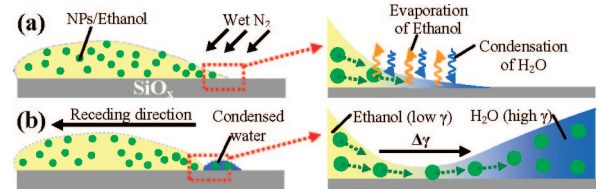

Figure 2. Schematic illustration of the self-assembly of NPs: (a) exposing a NP/ethanol suspension to a wet N_2 stream induces the evaporation of ethanol and the condensation of water near the three-phase contact line, which leads to a concentration gradient near the contact line; (b) the concentration gradient and the difference between the surface tensions of ethanol (γ_{EtOH} = 22 mN/m) and water (γ_{H_2O} = 72 mN/m) create a surface tension gradient, driving the NPs/water toward the receding contact line.

spherical capped droplet and assembled into a circular ring after drying (Figure 1a inset and Figure S5). The ring formation is caused by the outward capillary flow induced by contact line pinning, which is known as the "coffee ring" phenomenon.[2j,6]

On the wettable substrate (i.e., substrate B), as the NPs/ethanol suspension recedes, the condensed water near the contact line wets the substrate completely and produces a very thin water film (Figure S4). Due to the large surface tension gradient between the water film and the receding ethanol suspension and the fingering instability at the receding contact line, the NPs in the ethanol suspension quickly move toward and into the fingers and facilitate the growth of fingers into stripes. As water in and surrounding the stripes evaporates rapidly, the NPs in the stripes result in ordered dotted stripes.

It should be noted that the simultaneous evaporation of ethanol and condensation of water are necessary for the self-assembly of NPs into the hexagonal pattern. On substrate A, evaporating NP suspension in ethanol or water under dry N_2 (without water condensation) results in a random deposition of NPs (Figure S6). The regularity of hexagonal patterns depends on the orderliness of the instability fingerings at the contact line. The inter-ring spacing (λ) corresponds to the characteristic wavelength of the Marangoni

10.1021/ja801438u CCC: $40.75

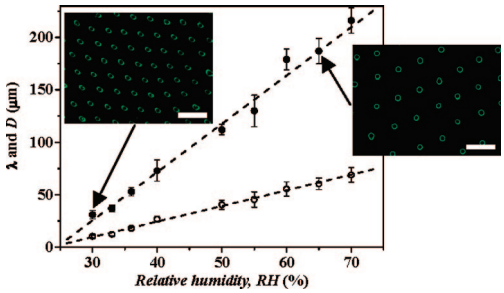

Figure 3. Inter-ring spacing or wavelength (λ, ●) (solid) and diameter of the ring (D, ○) can be readily controlled by relative humidity (RH, %) of the N_2 stream. The dashed lines are linear fittings. The fluorescent images illustrate two typical hexagonal ring patterns formed at a humidity of 30% ($\lambda \sim 30$ μm, $D \sim 10$ μm, scale bar = 50 μm) and 65% ($\lambda \sim 190$ μm, $D \sim 60$ μm, scale bar = 200 μm).

instability by $\lambda = 2\pi h/\alpha$, where h is the film thickness of the condensed water layer, and α is the dimensionless periodicity of the convection.[7] A reduction of water content (i.e., humidity) in the N_2 stream results in a decrease of condensed water near the contact line and hence its layer thickness (h). Figure 3 summarizes the inter-ring spacing, which is comparable to the calculated value (see Supporting Information), and ring size as a function of the humidity of the N_2 stream. The NP ring size depends not only on the size of the initiated water finger but also on the substrate property. On substrate A, the contact line of the water droplet does not self-pin, hence the droplet shrinks initially due to evaporation of water. As more NPs accumulate near the contact line due to the shrinkage, they deposit on the contact line and pin the contact line.[8] This perpetuated pinning leads to the formation of the coffee ring and thus determines the final size of the NP ring, which is much smaller than that of the initially formed water droplet (Figure S1). Nevertheless, the final ring size still decreases linearly with the humidity (Figure 3). Furthermore, the width of ring also decreases linearly with the humidity (Figure S3).

The coffee rings in hexagonal arrays have potential applications in the fabrication of a nanowire, patterning, and optical and electronic devices.[6c,9] However, the ring structure is undesired in other cases, for example, protein microarray.[10] Since the contact line pinning and water evaporation are two necessary conditions for the formation of the coffee ring, eliminating either of these two conditions will allow a uniform distribution of NPs throughout the entire circular base of the droplet.[2j,8b] Releasing pinning stress and preferable evaporation on the top of the droplet have both been attempted.[8b] However, releasing pinning normally results in a deviation of the circular shape, and preferable evaporation is difficult for a large amount of droplets.[8b] In this study, we attempt to obtain a uniform distribution by slowing the evaporation of water droplets. In particular, a 0.1 vol % of ethylene glycol is added into the ethanol suspension to reduce the evaporation rate of water.[11] Immediately after droplets form, the sample is kept under high humidity to further decrease the evaporation rate. The NPs within the droplets deposit onto the substrate slowly (~20 min), which leads to uniform distributions of NPs within the circular bases of the droplets (Figure 4).

The pattern formed on substrate B also depends on the water content in the N_2 stream (Figure S7). Evaporation of NPs/ethanol suspension under a N_2 stream with a low humidity (RH < 30%) results in a thick NP film. The use of an intermediate humidity (40−70%) leads to dotted stripes, while the use of a high RH

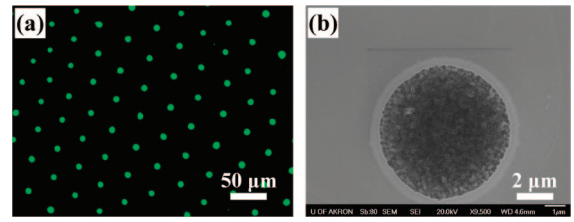

Figure 4. (a) Fluorescent microscopic image of a hexagonal NP pattern with a uniform distribution of the NPs within each circular patch. (b) SEM image of a uniform patch. RH of N_2 stream: 33%.

(~85%) produces a spokelike pattern. A possible reason could be that a thicker film of water condenses at a higher humidity and replaces the ethanol in the suspension after ethanol completely evaporates. Therefore, the pattern formed at a RH of ~85% is similar to that formed by drying the NPs/water suspension.[2e,g] More quantitative study is being carried out.

In summary, both hexagonal and stripelike patterns can be self-assembled on substrates with different wettability. This simple approach utilizing the combined evaporation of ethanol and condensation of water followed with Marangoni flow opens a new avenue for fabricating ordered NP patterns in a controllable and cost-effective manner. The patterns can be ideal templates for studying protein immobilization, cell/bacterial adhesion, and biosensor and medical assays.

Supporting Information Available: Additional experimental details and figures are included. This material is available free of charge via the Internet at http://pubs.acs.org.

References

(1) (a) Whitesides, G. M.; Grzybowski, B. *Science* **2002**, *295*, 2418–2421. (b) Holtz, J. H.; Asher, S. A. *Nature* **1997**, *389*, 829–832. (c) Kobayashi, N.; Egami, C. *Opt. Lett.* **2005**, *30*, 299–301. (d) Vlasov, Y. A.; Bo, X.-Z.; Sturm, J. C.; Norris, D. J. *Nature* **2001**, *414*, 289–293.

(2) (a) Xia, D.; Brueck, S. R. J. *Nano Lett.* **2004**, *4*, 1295–1299. (b) Amos, F. F.; Morin, S. A.; Streifer, J. A.; Hamers, R. J.; Jin, S. *J. Am. Chem. Soc.* **2007**, *129*, 14296–14302. (c) Kalsin, A. M.; Fialkowski, M.; Paszewski, M.; Smoukov, S. K.; Bishop, K. J. M.; Grzybowski, B. A. *Science* **2006**, *312*, 420–424. (d) Yin, Y.; Lu, Y.; Gates, B.; Xia, Y. *J. Am. Chem. Soc.* **2001**, *123*, 8718–8729. (e) Xu, J.; Xia, J.; Lin, Z. *Angew. Chem., Int. Ed.* **2007**, *46*, 1860–1863. (f) Malaquin, L.; Kraus, T.; Schmid, H.; Delamarche, E.; Wolf, H. *Langmuir* **2007**, *23*, 11513–11521. (g) Huang, J.; Kim, F.; Tao, A. R.; Connor, S.; Yang, P. *Nat. Mater.* **2005**, *4*, 896–900. (h) Huang, J.; Tao, A. R.; Connor, S.; He, R.; Yang, P. *Nano Lett.* **2006**, *6*, 524–529. (i) Bigioni, T. P.; Lin, X.-M.; Nguyen, T. T.; Corwin, E. I.; Witten, T. A.; Jaeger, H. M. *Nat. Mater.* **2006**, *5*, 265–270. (j) Deegan, R. D.; Bakajin, O.; Dupont, T. F.; Huber, G.; Nagel, S. R.; Witten, T. A. *Nature* **1997**, *389*, 827–829. (k) Brinker, C. J.; Lu, Y.; Sellinger, A.; Fan, H. *Adv. Mater.* **1999**, *11*, 579–585.

(3) (a) Suematsu, N. J.; Ogawa, Y.; Yamamoto, Y.; Yamaguchi, T. *J. Colloid Interface Sci.* **2007**, *310*, 648–652. (b) Martin, C. P.; Blunt, M. O.; Pauliac-Vaujour, E.; Stannard, A.; Moriarty, P.; Vancea, I.; Thiele, U. *Phys. Rev. Lett.* **2007**, *99*, 116103/1–116103/4.

(4) (a) Vuilleumier, R.; Ego, V.; Neltner, L.; Cazabat, A. M. *Langmuir* **1995**, *11*, 4117–4121. (b) Fanton, X.; Cazabat, A. M. *Langmuir* **1998**, *14*, 2554–2561.

(5) Karthaus, O.; Grasjo, L.; Maruyama, N.; Shimomura, M. *Chaos* **1999**, *9*, 308–314.

(6) (a) Hu, H.; Larson, R. G. *Langmuir* **2005**, *21*, 3963–3971. (b) Hu, H.; Larson, R. G. *Langmuir* **2005**, *21*, 3972–3971. (c) Hu, H.; Larson, R. G. *J. Phys. Chem. B* **2006**, *110*, 7090–7094. (d) Bormashenko, E.; Bormashenko, Y.; Pogreb, R.; Stanevsky, O.; Whyman, G. *J. Colloid Interface Sci.* **2007**, *306*, 128–132.

(7) Maillard, M.; Motte, L.; Pileni, M. P. *Adv. Mater.* **2001**, *13*, 200–204.

(8) (a) Deegan, R. D.; Bakajin, O.; Dupont, T. F.; Huber, G.; Nagel, S. R.; Witten, T. A. *Phys. Rev. E* **2000**, *62*, 756–765. (b) Deegan, R. D. *Phys. Rev. E* **2000**, *61*, 475485.

(9) (a) McLellan, J. M.; Geissler, M.; Xia, Y. *J. Am. Chem. Soc.* **2004**, *126*, 10830–10831. (b) Maenosono, S.; Dushkin, C. D.; Saita, S.; Yamaguchi, Y. *Langmuir* **1999**, *15*, 957–965.

(10) Deng, Y.; Zhu, X. Y.; Kienlen, T.; Guo, A. *J. Am. Chem. Soc.* **2006**, *128*, 2768–2769.

(11) Rusdi, M.; Moroi, Y.; Nakahara, H.; Shibata, O. *Langmuir* **2005**, *21*, 7308–7310.

JA801438U